

Primary Processes and Structure of the Photosystem II Reaction Center. 4. Low-Intensity Femtosecond Transient Absorption Spectra of D1-D2-cyt-b559 Reaction Centers^{†,‡}

Marc G. Müller, Mathias Hucke, Michael Reus, and Alfred R. Holzwarth*

Max-Planck-Institut für Strahlenchemie, Stiftstr. 34–36, D-45470 Mülheim a.d. Ruhr, Germany

Received: December 11, 1995; In Final Form: February 29, 1996[®]

Low-intensity transient absorption spectroscopy has been performed on the isolated D1-D2-cyt-b559 reaction center complex of photosystem II from spinach. The excitation intensity was low enough to keep annihilation at a relatively low level ($\sim 11\%$) and still maintain a very high signal/noise ratio. The kinetics has been measured with ~ 200 fs resolution over two time ranges extending up to 200 ps for two different excitation wavelengths (680 nm, preferential primary donor excitation, and 670 nm, preferential external chlorophyll excitation). Detection wavelengths both in the pheophytin Q_x region (535–555 nm) and in the chlorin Q_y region, including the stimulated emission range (660–760 nm) have been employed. The data for all excitation/detection wavelength pairs and from both time ranges have been analyzed by combined global analysis. A highly complex kinetics, i.e. six lifetimes, has been found necessary for a good description of the data over the entire excitation/detection matrix and time range. These lifetimes are $T_1 = 2.4 \pm 0.3$ ps, $T_2 = 8.9 \pm 1$ ps, $T_3 = 19.8 \pm 3$ ps, $T_4 = 56 \pm 10$ ps, and $T_5 \geq 1$ ns (long-lived, nondecaying). The fastest component (T_6) in these fits had an ca. 300 ± 50 fs lifetime. Decay-associated spectra of these components are presented for both excitation wavelengths. In a preliminary analysis the 2.4 ps component is assigned to primary charge separation; the 8.9 and 19.8 ps components, to slow energy transfer from external chlorophylls; and the 56 ps component, to a relaxation process among different radical pairs. The ultrafast component most likely reflects the excited-state equilibration within the reaction center core. This assignment is supported by a minimal—yet incomplete—kinetic model which provides rate constants and species-associated difference spectra for the intermediates. In this modeling the *apparent* rate constant for primary charge separation from the excited reaction center core is 120 ± 30 ns⁻¹. In this minimal kinetic model the formation of the primary radical pair occurs exclusively with a 2.8 ps lifetime. Two radical pair states and two external chlorophylls have to be included in the minimal kinetic model for a reasonable description of the data. The data is compared with transient absorption data from other groups and with the results from our previously reported fluorescence study. The high *apparent* rate constant of 120 ns⁻¹ for charge separation found in the kinetic models as well as other data exclude the possibility that primary charge separation could be associated primarily with a ~ 21 ps lifetime.

Introduction

The reaction center (RC) of photosystem (PS) II, the so-called D1-D2-cyt-b559 complex, was isolated for the first time now nearly 10 years ago.^{1,2} It contains the D1 and D2 polypeptides and the apoproteins of cytochrome *b*-559.^{1,3} The D1 and D2 polypeptides of the PSII RC complex have significant homology with the L and M subunits of purple bacterial RCs, respectively.^{4–6} The primary electron donor is P680, presumably a special pair of chlorophyll (Chl) *a* analogous to the one in purple bacteria.⁷

There exists an agreement now between most groups that typical preparations of the D1-D2 complex obtained in various laboratories show a Chl content between 6 and 7 Chl/2 Pheo.^{8,9,45} This means that in addition to an RC core which most probably has a pigment content analogous to that of bacterial RCs, i.e. 4 Chl *a* and 2 Pheo *a*,^{6,7} the D1-D2 complex contains at least two

additional Chls. It has been suggested that these additional Chls are located at the periphery of the complex and that they transfer their energy slowly to the RC core and to P680.^{10–13} The absorption spectrum of the D1-D2-cyt-b559 complex is highly congested with the Q_y bands of all pigments overlapping strongly. Unlike the situation in purple bacterial RCs, where the primary donor state is populated after excitation almost exclusively, in D1-D2 complexes several almost isoenergetic excited states exist whose kinetics has to be taken into account. Furthermore inhomogeneous broadening of states is of the same order as the spectral separation of the individual pigments.^{14–16} All this provides a major difficulty for the interpretation of optical spectroscopic data. Konermann and Holzwarth recently analyzed the D1-D2 absorption spectrum in detail within the framework of a weak coupling between all pigments, taking into account both electron–phonon coupling and inhomogeneous broadening.¹⁶ An alternative model, assuming substantial exciton interaction among all the RC core pigments, has been suggested recently as well.¹⁷

The kinetics of the primary processes in the D1-D2 complex have attracted much attention. From the first ultrafast transient absorption data on the isolated D1-D2 complex Wasielewski and co-workers proposed a charge separation time of about 3 ps at higher temperatures¹⁸ and even faster, i.e. 1.4 ps, at 15 K.¹⁹ The 3 ps charge separation time was in good agreement with an early extrapolation by Schatz et al.^{20,21} based on

* Author to whom all correspondence should be addressed.

[†] This work has been presented in part at the ESF-Workshop on “Structure and Function of the isolated D1-D2 reaction center”, Wye College, England, April, 1995, and at the workshop on “Electron transfer processes in photosynthesis and artificial systems”, Jyväskylä, Finland, December, 1994.

[‡] Abbreviations: Chl, chlorophyll; Pheo, pheophytin; RC, reaction center; D1, D2, polypeptides of the reaction center of photosystem II; DADS, decay-associated difference spectrum; SADS, species-associated difference spectrum.

[®] Abstract published in *Advance ACS Abstracts*, May 1, 1996.

fluorescence kinetic data from intact PS II particles. Roelofs et al.,¹¹ studying the primary events by picosecond fluorescence reported a dominant 1–6 ps component⁴⁶ in the kinetics which was attributed to the primary charge separation¹¹ and in addition also a slow energy transfer in the 20–30 ps region.^{10,11} Very similar results were reported by us later on a so-called “6 Chl prep”²² which is now standard in most laboratories. In these measurements, when carried out with selective P680 excitation, a 3 ± 1 ps main component was assigned to the effective primary charge separation process while the slow ca. 20 ps component showed a more red-shifted emission spectrum, thus identifying it as an energy-transfer component from/to some long-wave Chl. Upon selective excitation of blue pigments (around 660 nm) an additional energy transfer component of about 5–8 ps was found. In low-temperature fluorescence measurements even more pronounced slow energy-transfer components were detected.^{10,11} In a recent more extensive fluorescence kinetic study we found a complex kinetics with lifetimes of 3, 8, 12, and 26 ps and some additional long-lived components.¹³ From these data Holzwarth and co-workers^{13,22} concluded that (i) the fastest and dominant *effective* charge separation lifetime in the D1-D2 RC should be $\sim 3 \pm 1$ ps, (ii) that the lifetimes of ~ 8 ps (upon blue excitation), 12 ps, and 26 ps represented energy transfer times from the external Chls, and (iii) that the Pheo⁻ formation observed with a time constant of ~ 20 ps²³ should actually be interpreted as being limited by the slow energy transfer from some of the external Chl(s) to the RC core. This interpretation is in general agreement with a transient absorption study by Schelvis et al.¹² and also with earlier hole burning data on the D1–D2 complex by Small et al.^{15,24} Our recent fluorescence study suggests that an ~ 55 ps component is associated with a relaxation between different radical pairs.¹³

The most extensive femtosecond transient absorption studies so far have been carried out by the group of Klug et al. (see e.g. refs 23 and 25–27) using various excitation wavelengths and measuring detailed kinetic spectra. In summary, they found components of 3.5 ps, 15–27 ps, and long-lived component(s) in their transient absorption data (additional subpicosecond components were also found and were interpreted as reflecting ultrafast energy-transfer components in the RC core²⁸). Although the set of lifetimes which Klug and co-workers found in their transient absorption data is fairly consistent with the set of lifetimes we found by fluorescence,⁴⁷ they interpreted their data in quite a different way: They (i) assigned a 21 ps component to “...reflect the effective charge separation process, not limited by a slow energy transfer step...”,²⁷ (ii) suggested that an additional energy-transfer step may slow down this lifetime to 27 ps when exciting in the 670 nm region,²⁷ and (iii) claimed that our conclusions drawn from fluorescence data “...were not consistent with (their) femtosecond absorption data...”.²⁵ In essence that assignment is largely based on the appearance kinetics of Pheo⁻ at 543 and 460 nm^{23,26} on the one hand and the decay of stimulated emission above 700 nm²⁵ on the other hand, which were both found to occur primarily with a lifetime of about 21 ps. Notably the 3.5 ps component was not assigned to any specific process so far.²⁵

These mutually exclusive interpretations of the kinetics of primary events by the different groups may have several reasons. First, there might actually exist a real difference in the samples between the various groups. We consider this not as the most likely cause of the discrepancy, however, since despite some minor differences in the data they agree within the error limits and the respective S/N ratios. It should be noted, however, that up to now none of the groups working in this field has presented

a detailed kinetic model that would fully and satisfactorily explain the transient absorption data. Without such a model any conclusive statements about the origin of the complex transient absorption components is quite uncertain, however. Second, transient absorption spectroscopy and fluorescence kinetics has so far not been carried out under comparable low-intensity excitation conditions. For example, we have shown recently that under the excitation conditions that have been used so far for transient absorption measurements on the D1-D2 complex considerable intensity effects on both the kinetics and the yield of radical pair formation occur due to efficient annihilation processes.²⁹ In view of the extremely complex kinetics of the primary processes in the D1-D2 complex it is highly desirable to apply several different and complementary techniques under comparable excitation intensities. We therefore have started a program to study both fluorescence and transient absorption kinetics under similar low-intensity excitation conditions. One of the essential aspects of these studies will be the use of a range of different excitation wavelengths and temperatures. An extensive fluorescence kinetic study, presenting also a preliminary kinetic model, has been finished recently.¹³ We now report the transient absorption counterpart with femtosecond resolution. The aim of this study is several-fold: (i) to present an extensive data set with different excitation and a range of detection wavelengths obtained under low-intensity excitation, thus avoiding as much as possible annihilation effects; (ii) to compare these data both to the transient absorption data of other groups and also to our own fluorescence kinetics; and (iii) to develop a first, though simplified, kinetic model, based entirely on transient absorption, which can be compared to the one we obtained from fluorescence.¹³ In this way a broader basis could be developed which eventually might allow us to present a final refined model for the kinetics of the primary processes in the D1-D2 complex.

Materials and Methods

Sample. The D1-D2-cyt-b559 RCs used in this work have been isolated according to van Leeuwen et al.³⁰ with slight modifications.¹⁶ For these measurements a large amount of sample was required. In view of possible subtle differences in the kinetics from different preparations (which were shown for example to vary slightly in the Chl content¹⁶) we intended to do all measurements on exactly the same material. Thus the RCs from several independent isolation runs, each yielding a Chl/2 Pheo ratio in the range of about 6.0–6.3 were pooled and combined to obtain a large sample pool. Before combining samples from different preparations the 4.2 K absorption spectra and HPLC pigment determination were carried out on every sample. Only such samples that fell into a narrow range of pigment content and had very similar 4.2 K absorption was included in the pool (see ref 16). All measurements reported here have been carried out on fractions of that pool which had a Chl/2 Pheo ratio of 6.1 ± 0.2 as determined by HPLC.¹⁶ After pooling the reaction centers were shock frozen at 77 K in caps containing the approximate amount required for one measurement. The room temperature and 4 K absorption spectra of these RCs are shown in Figure 1. For measurements the sample was contained in buffer Tris-HCl 50 mM, pH = 7.2, detergent dodecyl maltoside 0.1%. The sample was contained in a rotating cuvette (pathlength $d = 1$ mm, volume 3 mL) that was cooled to 4 °C. The cuvette was both rotated and slowly horizontally shifted so that on average the same spot in the cuvette would see the next laser pulse only after ≥ 50 s. The cuvette was air tight so that with the additional use of the enzymatic oxygen-scrambling system glucose/glucoseoxidase and catalase³¹ the

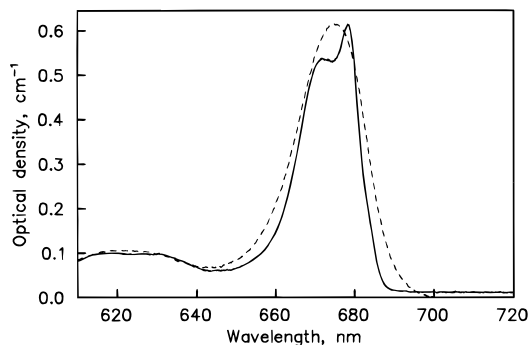


Figure 1. Room temperature (dashed) and 77K (full line) absorption spectra of the D1-D2 RCs used in this study. For the 77K spectrum the sample had been mixed with glycerol to a final concentration of 60% v/v glycerol.

sample was kept under anaerobic conditions. The absorption of the sample at the excitation wavelength was adjusted to about 0.8/mm.

Femtosecond Absorption and Data Analysis. Excitation pulses for femtosecond absorption measurements were generated by chirped pulse amplification of 40 fs pulses from a Ti-sapphire laser oscillator (Tsunami, Spectra Physics) in a regenerative amplifier and stretcher/compressor unit (Quantronix). The output pulses from the amplifier (FWHM = 80 fs) were frequency shifted using an optical parametric generator (Topas, Light Conversion). The spectral width of the excitation pulses (~ 120 fs FWHM, ca. 180 fs autocorrelation width) was ≤ 6 nm (FWHM) at a repetition rate of 3 kHz. Thus the pulses were close to being transform limited. Part of the 800 nm light from the amplifier was used to generate a white light continuum of 80 fs width (FWHM). The pump and probe pulses were polarized at magic angle relative to each other in order to exclude any kinetic depolarization effects. The rms noise of the detection system was as low as $\pm 5 \times 10^{-7}$ OD units under actual measurement conditions in the best cases. The detection system was the same as described shortly in ref 29 and full details will be reported in a separate paper.

Data Analysis. Data were analyzed in a global fashion by combining the data sets recorded at all excitation/detection wavelength pairs and at two different time resolutions and time ranges over which the data have been measured (equal weighting of the two time ranges). In this way decay-associated difference spectra (DADS) and a global set of lifetimes have been obtained.^{32,33} The global analysis included a deconvolution of the kinetics with the autocorrelation of the excitation pulse although this was not absolutely required for resolving lifetimes above 200 fs in view of the very narrow excitation pulse. In principle the deconvolution ought to be carried out with the cross-correlation function of the excitation and the probe pulse. We checked however that there was no significant difference to the autocorrelation trace and ensured that only for extremely short lifetimes (≤ 100 fs) a more sophisticated procedure would be required. In addition global target analysis has been performed on the output from the combined global analysis (lifetimes and DADS) in order to test various kinetic models. The results of this analysis are the rate constants of the model and the species-associated difference spectra (SADS) of the species present in the model.^{32,33} The quality of the fits was judged in each case on the basis of χ^2 values and plots of the weighted residuals.³³ Note that in the target analysis the aim is not to reproduce exactly the lifetimes obtained experimentally. Rather the target function is optimized to optimally reproduce the time course of the signal at each wavelength, which does not necessarily require exactly the lifetimes obtained experi-

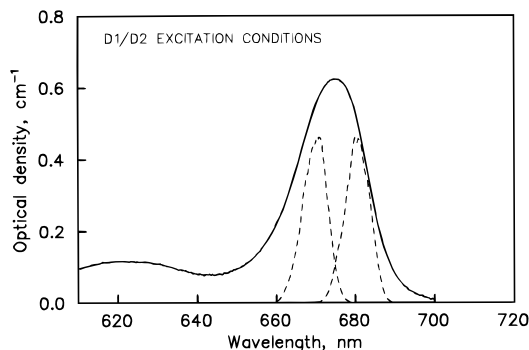


Figure 2. Room temperature absorption overlaid with the spectra of the femtosecond excitation pulses (dashed) for the two different excitation wavelengths (670 and 680 nm) used in this work.

mentally, although in the simplest cases these two aims are congruent.³³ This form of the target analysis gives more freedom in the choice of kinetic models as compared to a form where the lifetimes themselves should be reproduced as closely as possible. This distinction is important when comparing the experimentally obtained lifetimes (from the global analysis) and the lifetimes resulting from the kinetic model.

Results

Transient Absorption Data. Prior to the measurements reported here we have carried out an extensive excitation intensity-dependence study of the kinetics from D1-D2 RCs which revealed the occurrence of annihilation processes even down to an excitation density of about 10^{13} photons cm^{-2} pulse $^{-1}$ (at 680 nm). It was found that the amount of radical pair formation followed an intensity dependence that was in agreement with that expected from an efficient singlet annihilation process.²⁹ In the present measurements the excitation pulse energy was low enough that annihilation effects on the kinetics can be largely ignored although they are not completely absent (about 11% annihilation still persists²⁹). To our knowledge these are the lowest intensity absorption measurements performed so far on the D1-D2 complex (for a detailed discussion see ref 29). Excitation intensities of 7 nJ/pulse corresponding to a photon density of $\sim 1.8 \times 10^{14}$ photon cm^{-2} pulse $^{-1}$ at the excitation wavelengths of 670 and 680 nm were used in this study. Under these conditions the excitation probability per RC complex and pulse is 0.23.²⁹ Measurements with the required high S/N ratio at such a low excitation intensity were only possible due to the fact that our detection system has an extremely low noise level.

Figure 2 shows the room temperature absorption spectrum of the D1-D2 complex overlaid with the spectra of the femtosecond excitation pulses at the two excitation wavelengths. These wavelengths were chosen such that with 680 nm we expect an optimal excitation selection for P680 (or the RC core)¹⁶ and at 670 nm we expect a more specific excitation of one of the external Chls (we call this the "blue Chl"¹⁶). In this study we intentionally avoided excitation beyond 680 nm since this would in our view lead to a more pronounced excitation of the so-called external "red Chl".¹³

Transient absorption kinetics were measured for two excitation wavelengths and detection both in the 535–555 nm range and in the 660–700 nm range (every 5 nm). In addition the kinetics were measured at 730 and 760 nm. For each excitation/detection wavelength pair two time ranges were measured: The first set covered a total range of 50 ps and the second one a range of 200 ps. We show here only the data in the short time range since essentially all the important energy transfer and

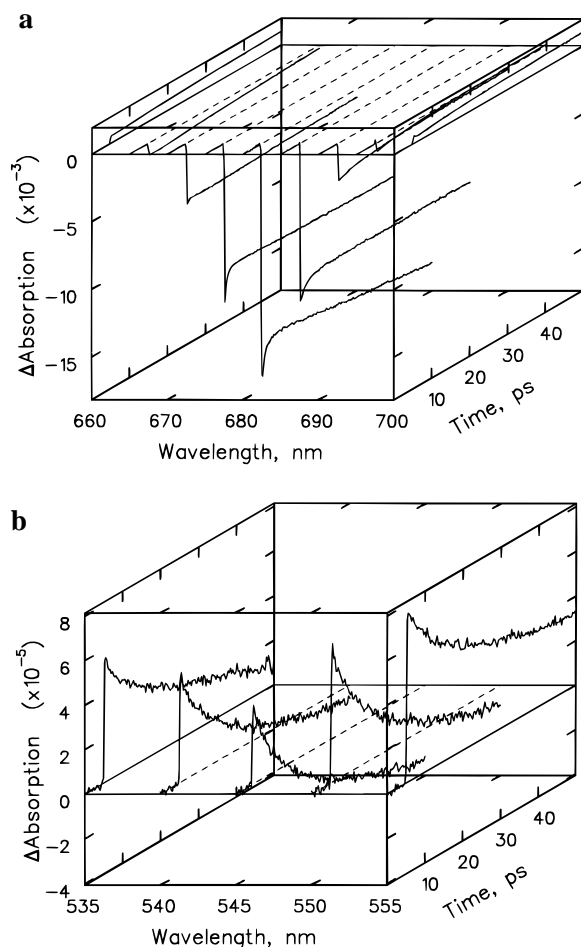


Figure 3. Femtosecond transient absorption decays (short time range) measured upon low intensity excitation at 680 nm: (a) 660–700 nm range and (b) 535–555 nm detection range.

charge separation kinetics occurs in that range. The data in the longer time range (not shown) are essential however to allow a good separation and resolution of the long-lived and the short-lived components in the global analysis. Figure 3 shows the original transient absorption data obtained for an excitation wavelength of 680 nm for the long-wavelength (Figure 3a) and the short-wavelength (Figure 3b) detection ranges. The corresponding data for excitation at 670 nm are shown in Figure 4. Note that in Figure 3b (680 nm excitation) for 545 nm detection the signal crosses zero at about 10 ps delay, whereas for 670 nm excitation (Figure 4b) the zero crossing time is shifted to about 20 ps. Figure 5 compares the kinetic traces for 730 and 760 nm detection for both excitation wavelengths, respectively.

Global Lifetime Analysis. All the data were analyzed globally in terms of a sum-of-exponentials kinetic function. For a good description of the data across the whole excitation/detection range (data from 670 and 680 nm excitation fitted together) and the maximal time window of 200 ps (i.e. including both measurement ranges) a sum of six exponentials was necessary (all lifetimes are collected in Table 1). With five exponentials significant systematic deviations occurred in the residuals plots of many excitation/detection wavelength pairs (data not shown, the corresponding lifetimes of the five-exponential fit were $T_1 = 1.6 \pm 0.3$ ps, $T_2 = 15 \pm 2$ ps, $T_3 = 50 \pm 5$ ps, $T_4 \geq 1$ ns, and $T_5 = 200 \pm 50$ fs). The lifetimes of the components above 1 ps from the combined global analysis in the optimal six-exponential fit were $T_1 = 2.4 \pm 0.3$ ps, $T_2 = 8.9 \pm 1$ ps, $T_3 = 19.8 \pm 3$ ps, $T_4 = 56 \pm 10$ ps, and $T_5 \geq 1$ ns (the latter lifetime is not determined well on the maximal time window of 200 ps as used here). The fastest component (T_6)

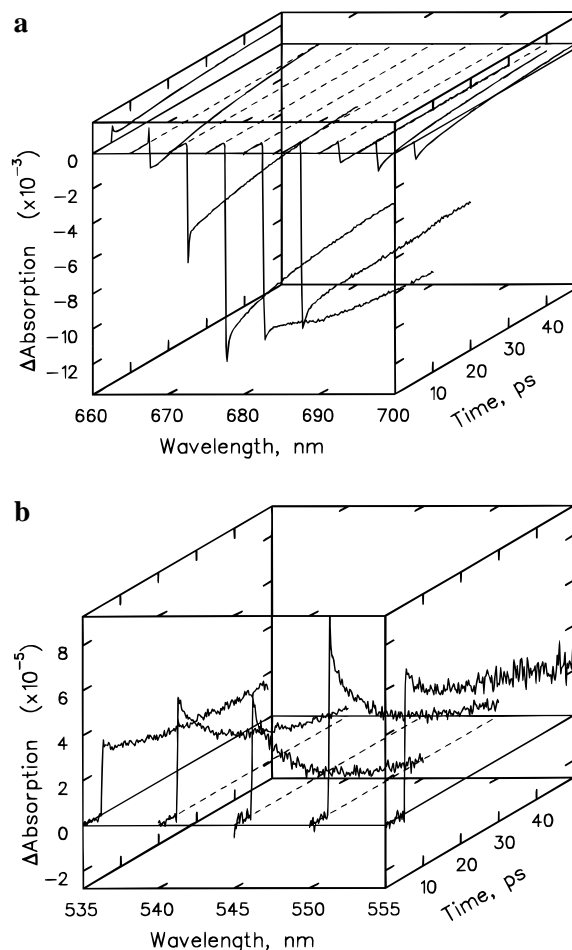


Figure 4. Femtosecond transient absorption decays (short time range) measured upon low intensity excitation at 670 nm: (a) 660–700 nm range and (b) 535–555 nm detection range.

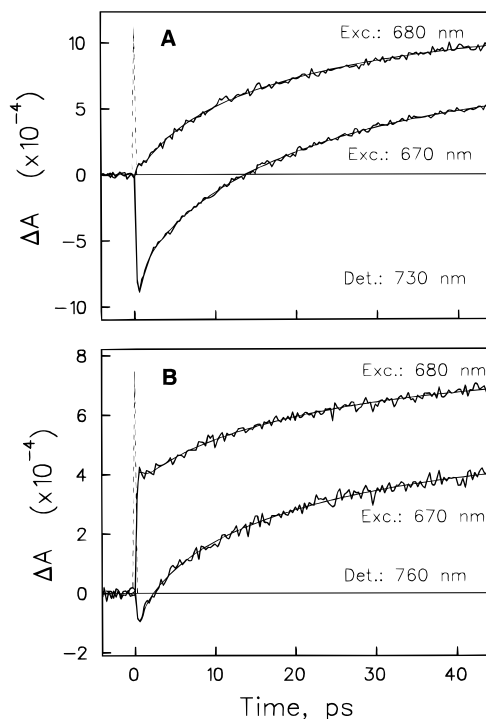


Figure 5. Femtosecond transient absorption decays at 730 (a) and 760 nm (b) for 680 and 670 nm excitation, respectively.

in these fits had a $\sim 300 \pm 50$ fs lifetime. Although this ultrafast component was necessary and included in all fits, it will not be

TABLE 1: Lifetimes from Global Analysis of Femtosecond Measurements Analyzed under Various Conditions^a

condition	T_1 , ps	T_2 , ps	T_3 , ps	T_4 , ps	T_5 , ns	T_6 , fs
global analysis of 670 nm excitation data	1.8 ± 0.3	6 ± 1	14.8 ± 2	45 ± 10	≥ 1	200 ± 50
global analysis of 680 nm excitation data	2.7 ± 0.3	8.5 ± 1	19.1 ± 2	55 ± 10	≥ 1	300 ± 50
combined global analysis of 670 nm and 680 nm excitation data; five exponentials	1.6 ± 0.3	—	15 ± 2	50 ± 5	≥ 1	200 ± 50
combined global analysis 670 nm and 680 nm excitation data; six exponentials	2.4 ± 0.3	8.9 ± 1	19.8 ± 3	56 ± 10	≥ 1	300 ± 50

^a All analyses were carried out by combining the short- and long-time range data sets in the same analysis (see text).

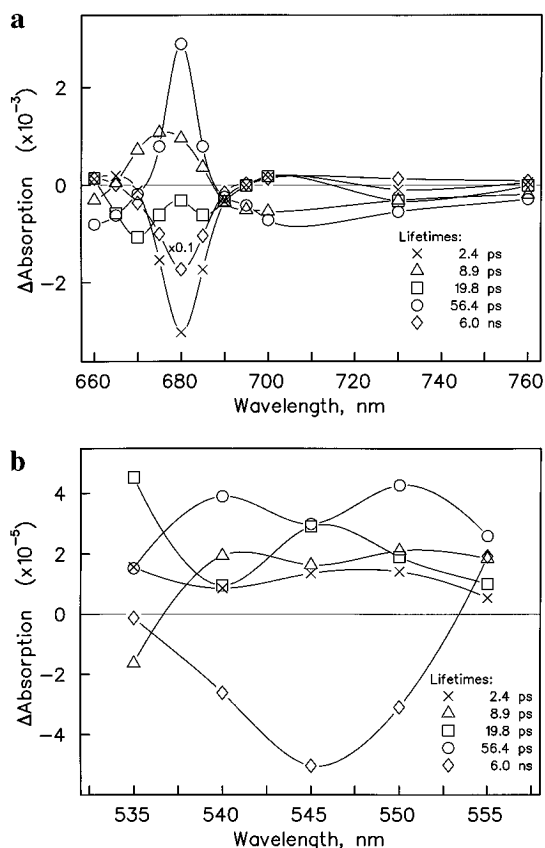


Figure 6. Decay-associated difference spectra (DADS) from global analysis of the 680 nm excitation data set taken over two time ranges: (a) 660–760 nm detection range and (b) 535–555 nm detection range. Note that the amplitude of the long-lived (nondecaying) component has been suppressed by a factor of 10 in order to better present the other components.

shown for two reasons: First, we do not intend to characterize in this work the subpicosecond kinetics but only components above ~ 1 ps. The rationale for this approach is the finding that the ultrafast (subpicosecond) processes correspond to an equilibration among the RC core pigments.³⁴ For a full characterization of the subpicosecond kinetics more detailed high-resolution data will be required in the future. Thus, we do not in this work interpret the ultrafast component in physical terms but for the time being we include it as a mere mathematical fitting parameter to describe the data. It cannot be left out of the data analysis, however, since this would cause a severe distortion of the short picosecond lifetimes and spectra. The DADS resulting from this analysis are shown in Figures 6 and 7 for excitation wavelengths of 680 nm and 670 nm, respectively.

Discussion

Excitation of 680 nm (Figure 6). Since the maximal absorption of the primary donor is believed to be located at 680 nm (see ref 35 for a review), that excitation wavelength should yield the highest proportion of RC core excitation, in agreement with our spectral analysis.¹⁶ The long-lived (non-

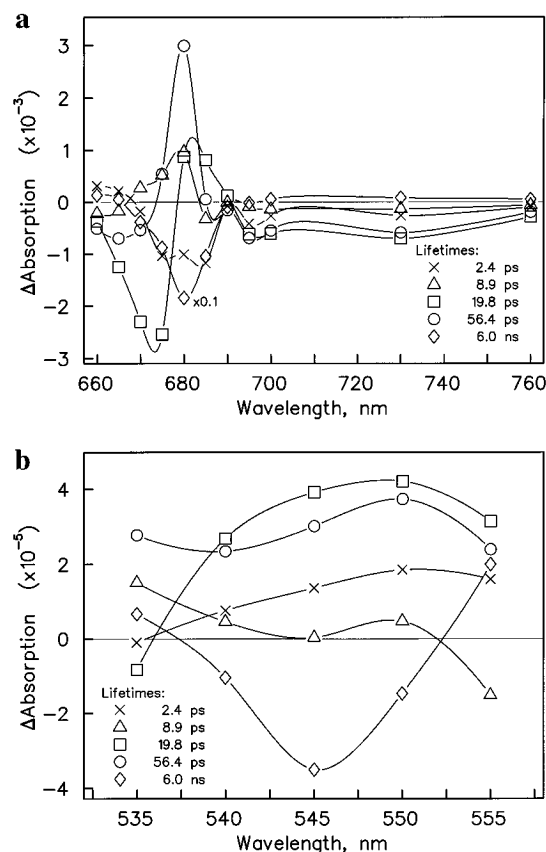


Figure 7. Decay-associated difference spectra (DADS) from global analysis of the 670 nm excitation data set taken over two time ranges: (a) 660–760 nm detection range and (b) 535–555 nm detection range. Note that the amplitude of the long-lived (nondecaying) component has been suppressed by a factor of 10 in order to better present the other components.

decaying) component in the Q_y region (660–760 nm) (Figure 6a) is in good agreement with published spectra^{23,36,37} and can thus be assigned to the radical pair spectrum ≥ 200 ps after the flash. The 545 nm region (Figure 6b) is expected to show strong contributions from the pheophytin(s), although all the chromophores will contribute to some extent to the excited-state absorption in that region. The spectral shape of the long-lived component in the 545 nm region is again in good agreement with published spectra although the relative amplitude of the bleaching as compared to the 680 nm bleaching is by a factor of about 5–10 times smaller than reported by Hastings et al.²³ The reason for this difference is not entirely clear to us.⁴⁸ The 2.4 ps component in the Q_y region has only about 10% of the maximal amplitude of the bleaching of the long-lived component. Its bleaching maximum is located at 680–685 nm with a side band at 730 nm. Below 670 nm and at 760 nm it shows an absorption increase. In the 545 nm region this component shows a small positive amplitude with maximum at 550 nm. The 8.9 ps component shows amplitudes that are over the most part of the Q_y region opposite in sign to those of the 2.4 ps component, except at 730 nm where both components show a bleaching. In the 545 nm region the relative absorption

changes for the 8.9 ps component are small. The 19.8 ps component shows bleaching bands (negative amplitude) at 670, 685, and 730 nm and is negative over most of the Q_y region. In the 545 nm range the spectrum is unstructured and shows a relatively large all-positive (absorption increase) contribution as does also the 56 ps component. The latter component in the Q_y region shows a relatively large positive component at 680 nm and a negative amplitude outside this region. The overall shape of this spectrum is similar to the radical pair spectrum but opposite in sign.

Excitation of 670 nm (Figure 7). At 670 nm excitation we except to excite more selectively one of the external Chls in the D1–D2 complex which have been shown to transfer energy slowly to the RC core.^{10,11,13,22,38} However the RC core, containing six chromophores, is still expected to be excited to a large extent at this wavelength. The spectrum of the long-lived component (Figure 7a) is basically identical as that with 680 nm excitation while the spectra of the other components depend quite substantially on excitation wavelength, except for the 56 ps component spectrum. The 2.4 ps component in the Q_y region shows minima at 675 and 685 nm and also around 700 nm. In the 545 nm region the corresponding spectrum shows a small absorption increase except at 535 nm where a small bleaching results. The 8.9 ps component in the 545 nm region shows a spectrum that is roughly opposite in sign to that of the 2.4 ps component. In the Q_y region the spectrum is wiggly and quite small. In contrast the 19.8 ps component shows relatively large amplitudes with a bleaching in the 660–675 nm range and a relatively large absorption increase around 680 nm. Above 700 nm also a moderate bleaching is observed. Overall the spectrum is quite different from that at 680 nm excitation. In the 545 nm region the 19.8 ps component shows a relatively large positive amplitude. The spectrum of the 56 ps component is essentially identical to that for 680 nm excitation across the entire detection wavelength range.

Tentative Assignment of Lifetime Components. In the past the observed kinetics in transient absorption experiments on D1–D2 has been discussed only in qualitative terms. Although it is important to try to deduce a qualitative assignment of components to physical processes (energy transfer, charge separation) directly from the raw data and the DADS and lifetimes, in a highly complex kinetic system the information gained from such an approach will be quite limited. The necessary analysis procedure in such a case must be kinetic modeling (see below). We will nevertheless give a short qualitative discussion here of some of the components. The rationale behind this is the fact that the DADS and lifetimes still represent in the most direct way the original data which should be comparable among different laboratories.

The only component that can be assigned unequivocally is the long-lived component which arises from the radical pair at long times. We should like to note, however, that even at about 200 ps after the flash we expect some contribution from excited states due to efficient back-reactions (up to 20%), as has been shown from our fluorescence analysis.¹³ The other component that can be assigned with good certainty is the 56 ps component. Its spectrum is roughly opposite in sign to the radical pair spectrum. We thus assign it to some relaxation between different radical pairs, i.e. the spectrum reflects the rise of the long-lived radical pair state. This assignment is in good agreement with the fluorescence kinetics where a radical pair relaxation component had approximately the same lifetime¹³ and—quite importantly—is also supported by the fact that the spectrum does not depend on the excitation wavelength, in

contrast to all shorter-lived components. The contribution of this component is quite large also in the 545 nm range.

The shapes of both the 19.8 and the 8.9 ps component depend quite strongly on the excitation wavelength. We thus assign these components tentatively to energy transfers from external Chls to the RC core. Such a principal assignment is strongly suggested from Figure 7a where the 19.8 ps component shows a negative/positive spectral feature generally characteristic for energy transfer. For the 8.9 ps component the assignment is less clear. We note however that these assignments to energy transfer are in good agreement again with the fluorescence analysis.¹³ Quite importantly, the 19.8 ps component at 700 and 760 nm is almost zero in amplitude for 680 nm excitation and differs substantially from the shape for 670 nm excitation, which clearly precludes its assignment to a component related to charge separation, since in that case one would expect (i) the rise in the relatively large absorption characteristics at long wavelengths for the radical pair, and (ii) a DADS that is independent of excitation wavelength. If this component is assigned to energy transfer however the vibrational side bands (in the region above 700 nm) of the energy donor and acceptor may roughly cancel and thus explain the small amplitudes in that range of the 19.8 ps component.

From the transient spectra alone the most difficult component to assign is the 2.4 ps one. For 680 nm excitation it represents a rapid loss of bleaching around 680 nm and its overall shape is somehow similar to a Chl excited-state difference spectrum. For 670 nm excitation this spectrum is more complex, however, and any qualitative assignment on the basis of its shape would be quite speculative in that case. If compared with our fluorescence analysis,¹³ the 2.4 ps component should reflect the primary charge separation. A somewhat surprising observation is the relatively small amplitude of the 2.4 ps component in the 545 nm range, which at first glance would seem to contradict its assignment to primary charge separation. If one were to assume another state between the excited core and the $P680^+Pheo^-$ radical pair state, however, then this observation could be reconciled easily with the data. That state would have to show relatively little bleaching of the 545 nm Pheo band. A transient $P680^+Chl^-$ intermediate state would be a possible candidate. In that case also a low amplitude of the 2.4 ps component would be expected around 545 nm. We note again that a definitive assignment of the various components can be only achieved on the basis of a detailed kinetic model (see below).

Comparison with Data from Other Groups. While some of the kinetic components observed in our experiments, in particular the ~ 3 ps component and one or more components in the range of 10–100 ps, are in general agreement with the data from Wasielewski and co-workers^{19,39} and Schelvis et al.,¹² a direct comparison is not possible since these groups did not measure or analyze detailed kinetic spectra. We note however, that some of the measurements of these groups are presumably strongly distorted due to multiple excitation effects of various kinds.²⁹ Such multiple excitation effects (singlet annihilation) may well explain the quite different kinetics in the 545 nm range (opposite sign) reported by Wiederrecht et al.⁴⁰ Also the kinetics in the 680 nm range reported by Schelvis et al.¹² differs in some important details from those found in our studies. For example the ratio of fast (3 ps) and longer-lived components is significantly larger in the data of Schelvis et al. than in our data at low intensity but is more in agreement with our high-intensity data at 680 nm.²⁹

The most extensive transient absorption data sets reported so far are those by the group of Klug and co-workers.^{23,25–27}

We thus compare now in detail our data to those results. We will concentrate mostly on the most recent data²⁶ also recorded under magic-angle detection conditions. Klug et al. found essentially four lifetimes with 100 fs, 3 ps, 21 ps, and a long-lived (nondecaying) component. We do not find a 100 fs component but rather a 300 fs component although our measurements would have allowed us to resolve at least components down to 100 fs. However, since the subpicosecond kinetics is most likely to be more complex than single-exponential we do not put much emphasis on this difference in lifetimes in the ultrafast component. We note however, that part of this shortening in the ultrafast lifetime and the corresponding large amplitude of this component might be caused by annihilation effects (see ref 29). On the basis of the absorption difference of the radical pair at 680 nm (long delay time) we can estimate that the measurements of Klug et al. have been performed at about 2–2.5 times higher equivalent excitation intensity (the excitation wavelengths in their and our experiments were in fact different but this has been taken into account in our calculation). Despite the higher excitation density used, most of the differences between our data (DAS and lifetimes) and those of Klug et al. are probably not primarily caused by annihilation but rather by the large differences in S/N ratio. As far as the probability for P680 (or rather RC core) excitation is concerned, their 694 nm excitation should be quite comparable to our 680 nm excitation (ignoring the slightly increased excitation probability for the red external Chl in their case), i.e. we expect preferential core excitation (≥ 70 –80%) under these conditions (see ref 16 for a detailed analysis of the absorption spectrum). The relative amplitude and the spectral shape of the 3 ps component in the data of refs 26 and 34 are in quite good agreement with the spectral shape and amplitude of our 2.4 ps component. Klug and co-workers found, in addition, a 21 ps component only while we required two additional components of 8.9 ps and 56 ps for a good fit. At first glance it might appear that the 21 ps in refs 26 and 34 and our 19.8 ps might be equivalent, reflecting the same process. Comparison of the associated spectra reveals, however, that they are very much different from each other. In fact it rather seems that the component most similar to their 21 ps component is our 56 ps component, although there are some distinct differences as well. The relationship thus is more complex. However, summing up the spectra of the 8.9, 19.8, and 56 ps components results in a spectrum that is in fact remarkably similar to that of the 21 ps component reported by Klug and co-workers.^{26,34} Also the weighted average of 8.9, 19.8, and 56 ps is reasonably close to 21 ps (the exact average lifetime depends on the wavelength range over which the averaging is performed). Thus the 21 ps component^{26,34} is clearly not the same as our 19.8 ps component. (The corresponding spectra are totally different; they are even opposite in sign around 680 nm.) Rather the 21 ps component is clearly a mixture of the three components resolved in our analysis. Since the origins of these three components in our data must be quite different (see above), this observation causes substantial doubts on the interpretation of Klug and co-workers as far as their assignment of the 21 ps component is concerned.^{23,25,26,34} The increased number of components required in our analysis is clearly caused by the much higher S/N ratio in our data as compared to previous work. Notwithstanding this difference in S/N ratios the data of refs 26 and 34 and our data most probably agree reasonably well in the Q_y region. For example at 730 nm and some other wavelengths the kinetics reported by Klug et al.²⁶ is very close to our kinetics (Figures 3a and 5a). Substantial differences exist however in the kinetics at 545 nm. For

example the ratio of positive (at zero time) to negative amplitude (above 50 ps) is about 4:1 in the data of Hastings et al.²³ while it is ≤ 1 :1 in our data (Figure 3b). We have discussed this discrepancy previously²⁹ and have proposed that it could be explained in the most reasonable way by annihilation effects caused by the use of higher excitation intensity for measuring the 545 nm range, which is a very low signal region.⁴⁹ In the most recent data measured also under magic-angle conditions²⁶ this ratio is somewhat reduced to about 2:1, but is still significantly higher than in our data. Summing up, the overall kinetics reported by Klug and co-workers for 694 nm excitation is probably quite similar to our kinetics for 680 nm excitation in the Q_y region, but not in the 545 nm region. However, the resolution into more components from our data is possible due to the substantially higher S/N ratio. For example at 730 and 545 nm the S/N ratio is about 2:1 in the data of Klug et al.²⁶ (similar in previous data) while it is at least 20:1 at 730 nm (Figure 5a) and still ≥ 10 :1 at the very small signals around 545 nm (Figures 3b and 4b) in our data. Ignoring at this point the large differences in S/N ratio, the raw data in their data and our data are likely to be quite similar (except for the 545 nm range). Thus any fundamental differences in the interpretation can hardly be justified on the basis of the data themselves. In this connection it must be noted, however, that Klug and co-workers in their interpretation put very strong emphasis on the kinetics in the 545 nm range where larger differences occur.

Kinetic Modeling. Given the situation discussed above extensive kinetic modeling of the data seems to be the only promising way to arrive at a valid and consistent interpretation. The aim of this kinetic modeling must be to obtain a set of rate constants that is (i) physically reasonable, (ii) provides a set of SADS that must agree in a reasonable way with known absorption difference spectra of Chl excited states and/or PS II radical pair states, and (iii) the relative absorption probabilities (excitation vector³³) of the different absorbing chromophores at the excitation wavelength should be consistent with the absorption spectra of the components.¹⁶ Only if all these conditions are fulfilled simultaneously can we accept a kinetic model to satisfactorily explain all aspects of the data. A further aim should be that the kinetic model and rate constants obtained from transient absorption data should be fully consistent with those from fluorescence kinetics. Most likely all these aims cannot be achieved in a single step given the complexity of the system. We thus choose to present here a first-order minimal kinetic model that describes well the fundamental behavior of the system but will require some refinement in the future.

Several kinetic schemes have been tested so far by target analysis on the data from the global analysis shown in Figures 6 and 7 (DADS and lifetimes). Note that the subpicosecond component(s) have not been included in these models since they are assumed to be due to rapid equilibration among the RC core pigments on a subpicosecond time scale.³⁴ We limit ourselves to straightforward rate equation models and ignore any possible rate distributions as discussed recently for purple bacterial RCs.⁴¹ Thus our present modeling included an excited and equilibrated RC core, one or two radical pair states, and one to three external Chls as the essential states or intermediates in the system. The choice of these models was directed on the one hand by the results from our analysis of picosecond fluorescence data¹³ and on the other hand by the complexity of the decay-associated difference spectra shown above. It is important to note that in the modeling we do not make any *a priori* assumptions about rate constants or spectral or lifetime assignments. In Figure 8 is the minimal kinetic scheme along with the corresponding optimized set of rate constants which best describes the data

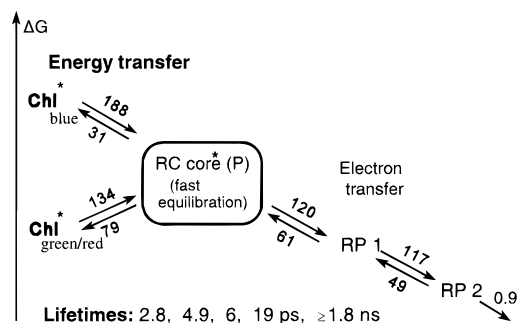


Figure 8. Minimal (first-order) kinetic model and rate constants suitable to describe the data from transient absorption measurements (see discussion for details). Chl_{blue} and $\text{Chl}_{\text{green/red}}$ denote the two external Chls. RP1 and RP2 are the two radical pairs. The recalculated lifetimes resulting from this model are shown at the bottom.

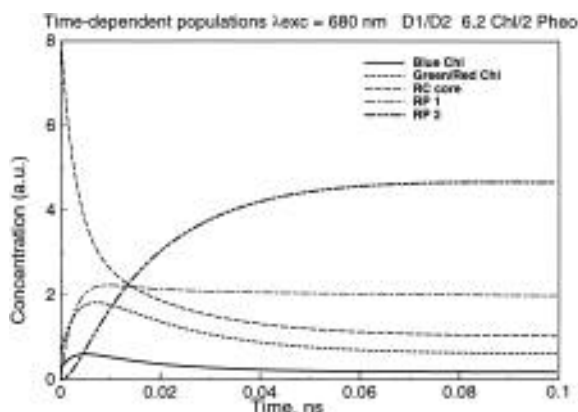


Figure 9. Plot of the populations of excited states and radical pairs vs time as obtained from the kinetic model in Figure 8 (see Table 2 for the exact mathematical description of the time dependence of the populations).

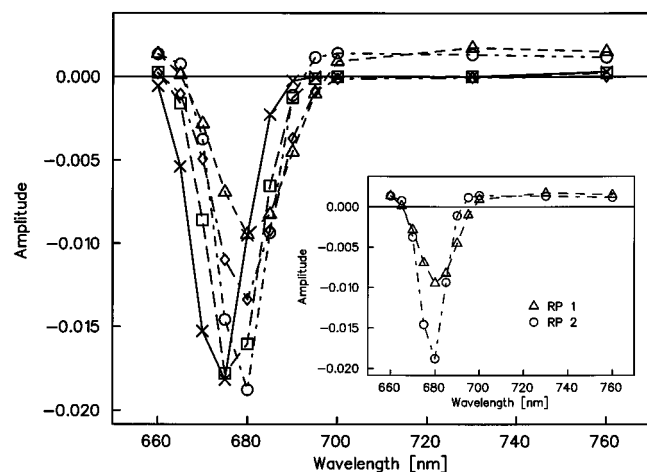


Figure 10. Species-associated difference spectra (SADS) resulting from the kinetic model shown in Figure 8. For the notation see caption to Figure 8: crosses, blue Chl; squares, green/red Chl; diamonds, RC core; triangles, RP1; circles, RP2. The inset shows separately only the spectra of the two radical pairs RP1 and RP2 for better clarity.

within the model assumptions stated above. The corresponding calculated time dependence of the concentration of the various intermediates is shown in Figure 9 and the results set of SADS is given in Figure 10. We have so far only included the data in the Q_y region in the kinetic modeling.

All our kinetic modeling performed so far reveals that in order to describe the main features of the kinetics and to avoid severe deviations from the experimental data at least two different radical pairs must be included in the kinetic scheme. We could

TABLE 2: Amplitude Components A_{ij} Describing the Time Dependence of Populations of Excited and Radical Pair Species of the D1-D2 Complex According to the Kinetic Model in Figure 8^{a,b}

lifetime	blue Chl	RC core	green/red Chl	RP 1	RP 2
2.8 ps	-0.079	0.432	-0.152	-0.322	0.122
4.9 ps	-0.011	0.005	-0.006	0.049	-0.038
6 ps	0.035	0.025	-0.060	0.049	-0.049
19 ps	0.053	0.232	0.226	0.014	-0.531
1.8 ns	0.018	0.107	0.063	0.209	0.496

^a Excitation vector ($\lambda_{\text{exc}} = 680$ nm) for the model is 0.016, 0.8, 0.07, 0.0, 0.0 for blue Chl, RC core, red/green Chl, RP 1, RP 2, respectively.

^b The population kinetics of species i is given by $c_i(t) = \sum_{j=1}^n A_{ij} \exp(t/\tau_j)$ where j denotes the n lifetimes τ_j .

not get any reasonable fit with one radical pair only. Furthermore at least two spectrally and kinetically distinct external Chls were required for reasonable fits. These findings are in good general agreement with the results from our fluorescence kinetic study.¹³ In this model (Figure 8) essentially all radical pair formation (i.e. $\text{RC core}^* \rightarrow \text{RP 1}$) is associated with a lifetime of ~ 3 ps. This can be seen in the most direct way in the plot of the time-dependent populations resulting from this kinetic scheme (shown in Figure 9). In this coupled kinetic scheme, in particular where several rates are similar, assignment of a particular lifetime to a particular process is not possible in a strict sense. Nevertheless the major process(es) contributing to a particular lifetime can be obtained from the kinetic matrix (amplitude components of lifetimes) of the model in Figure 8 which is given in Table 2. With these restrictions in mind the lifetimes of ~ 5 and 6 ps (in the model) reflect energy transfer times from the external Chls to the core and the ~ 19 ps component essentially reflects the transition from the primary to the secondary radical pair. As far as the spectra are concerned (Figure 10) the Chl with the fast energy transfer rate has a blue-shifted spectrum (*blue Chl*) as compared to the RC core and the other external Chl (*green/red Chl*). This is in good agreement with our fluorescence data and the spectral analysis which also indicated the presence of such a blue-shifted Chl^{13,16} at the same wavelength. Its excited state energy is located near 670 nm. The second Chl (*green/red Chl*) peaks around 678–680 nm. All the other SADS peak near 680 nm. Both Chls and the RC core have SADS which above 690 nm show spectral features which are more in agreement with an assignment to an excited state of Chls or Pheos (i.e. little excited-state absorption or even small bleaching).²⁵ In contrast the SADS assigned to the two radical pairs clearly show pronounced absorption increase above 690 nm as is characteristic for radical pairs. The SADS of RP1 is spectrally somewhat broader and much smaller in the 680 nm band and also differs slightly from that of RP2 above 690 nm. At present we are hesitant to give too much emphasis to these spectral differences between the two radical pairs since they might be caused at least in part by the simplicity of the model. In particular we cannot decide at present whether RP1 and RP2 reflect indeed different radical pairs or whether they may represent different protein conformations around the radical pair (e.g. relaxed radical pair model, see e.g. refs 13 and 42–44 for a discussion). The *effective* rate constant of charge separation (from the equilibrated RC core) in this model is ~ 120 ns⁻¹. This value is only slightly larger than the one obtained from the fluorescence kinetic modeling (about 110 ns⁻¹).¹³ Also the finding of a rather high charge recombination rate constant (61 ns⁻¹ in this model) is in general agreement with the modeling of the fluorescence data. We note in passing that the *effective* rate constant of 120 ns⁻¹ for charge separation in the model is consistent with an *intrinsic* rate constant of charge separation (for the hypothetical case that all excitation were

localized on P680) which is about three times higher, i.e. about 360 ns^{-1} which is very similar to the rate of charge separation for purple bacterial RCs. A detailed discussion of this point is given in ref 13 and will not be repeated here.

The present differences in rate constants between fluorescence and transient absorption models are not very large but still significant. They are clearly not caused by different lifetimes in fluorescence and transient absorption, which are in fact quite similar.¹³ Rather the differences in rate constants for charge separation and energy transfer are most probably caused by a somewhat different attribution of the fast process to energy transfer on the one hand and charge separation events on the other hand (note that the fastest energy transfer rate and the charge separation rate have similar values) in the two analyses. In particular some systematic errors in the energy transfer rates due to the choice of too simple a model will also influence the optimal charge separation rate constant in the two models somewhat differently.

Notwithstanding the fact that the minimal kinetic model presented here is able to explain quite well the principal features of the excited-state kinetics and the transient absorption spectra of the D1-D2 complex (Figures 6 and 7), we nevertheless do not consider this kinetic scheme as the final model for various reasons. First, we have evidence from both the spectral analysis¹⁶ and the fluorescence kinetics¹³ that actually three external Chls are present in the isolated D1-D2 complex. Accounting for that will make a refined model more complex and leaves several possibilities for the arrangement of these Chls in the kinetic schemes. Furthermore the spectral analysis provided evidence for the fact that the pigment composition is heterogeneous, i.e. at least one of these external Chls is present only in part of the RC complexes in the ensemble.¹⁶ This could explain for example why the 56 ps component is not reflected well in this model but is averaged to some extent with the 19.8 and 8 ps components. All these effects have not been accounted for in our present "first order" kinetic model. Other observations also indicate that the model presented in Figure 8 must be considered as a first-order approximation that needs refinement in the future. For example, the ratio of forward and backward rates for the energy transfer of the external Chls should in principle be related to the energy difference of the excited states of Chl and equilibrated core via the Boltzmann relationship if detailed balance is assumed. These energy differences can in principle be determined from the SADS. Although not largely off, in the present simple model these rate constant ratios are clearly not in full agreement with the measured energy differences, in particular for the green/red Chl (Figure 8). (For the green/red Chls we would expect a forward/backward ratio in rate constants of about 2.5:1 as compared to the ratio 1.7:1 in the model.) The reason for this mismatch is probably given by the fact that ignoring one of the external Chls will influence to some extent all the rate constants for the energy transfer in the model. This may also explain the difference in rate constant for charge separation in this simplified model as compared to our fluorescence kinetic analysis.¹³ Another drawback of this model at present is that in fact the 19 ps of the model actually shows the spectrum of the 56 ps components in the data (DADS). This clearly points to some unresolved mixing of kinetic components in the model and indicates that the final model should be complex, as indicated already by the optimal modeling for the fluorescence kinetics.¹³

Conclusions

Low-intensity femtosecond transient absorption measurements show that the overall kinetics of primary processes in the isolated

D1-D2 RC complex is substantially more complex than has been reported by other groups^{12,19,23,26} but is in very good agreement with our fluorescence data as far as the observed lifetimes and the general assignment of processes to lifetimes are concerned.¹³ Several of the previously reported femtosecond transient absorption data from other groups are substantially distorted by nonlinear annihilation effects or other multiple excitation artifacts.²⁹ We have been able to avoid such effects to a large extent in this study. However we should note that even in our low-intensity data some details of the kinetics and the spectra might still be slightly distorted due to the remaining annihilation effects.

Although the kinetic model presented here is still rather simple, all our kinetic modeling performed either on the transient absorption data reported here or on the fluorescence kinetics¹³ so far is consistent in the following two essential features: First, the primary charge separation, i.e. the formation of the primary radical pair, is primarily associated with the ~ 3 ps component. Second, components above 10 ps are either energy-transfer components from the external Chls or are associated with secondary radical pair processes. We thus exclude on the basis of our modeling the possibility that primary charge separation could be associated mainly with a ~ 21 ps component as proposed by Klug and co-workers.^{25,26} This possibility is already put into doubt by the mere fact that their 21 ps component is not a pure kinetic component but a mixture of at least three components ranging in lifetime from about 8 ps to about 56 ps and the further fact that the spectrum of the 21 ps component^{25,26} does not agree with the spectrum of our 19.8 ps DADS component.

In summary, in our view the fundamental discrepancies in the interpretation of the kinetic data from the D1-D2 complex are—besides effects caused by annihilation—mostly due to the previous lack of attempts to analyze the kinetic data in terms of suitable kinetic models.²⁶ In a system as complex as this the mere qualitative interpretation of the observed kinetics is likely to fail. It is very interesting in this connection to note that our minimal kinetic model with five components (Figures 8 and 10) is actually in excellent agreement with the kinetic and spectral analysis of Klug et al.^{23,26,34} but in clear disagreement with their interpretation. In our model the primary charge separation occurs with an *apparent* lifetime of ~ 3 ps while the 19 ps component (in the model) is associated with relaxation from the primary to the secondary radical pair. Since this model does not properly account for the prominent 56 ps component in our DADS due to averaging of lifetimes it needs to be extended to some extent in order to achieve an improved fit to our own data. This extension will not change the main features and results of the present model like the range of energy and charge separation rates, however.

Acknowledgment. We thank Mrs. I. Martin and Mr. U. Pieper for able technical assistance. Partial financial support has been provided by the Deutsche Forschungsgemeinschaft (Sonderforschungsbereich 189, Heinrich-Heine-Universität Düsseldorf and Max-Planck-Institut für Strahlenchemie, Mülheim a.d. Ruhr). We also thank Prof. K. Schaffner for support of this work.

References and Notes

- (1) Nanba, O.; Satoh, K. *Proc. Natl. Acad. Sci. U.S.A.* **1987**, *84*, 109.
- (2) Barber, J.; Chapman, D. J.; Telfer, A. *FEBS Lett.* **1987**, *220*, 67.
- (3) Chapman, D. J.; Gounaris, K.; Barber, J. *Biochim. Biophys. Acta* **1988**, *933*, 423.
- (4) Renger, G. *Photosynth. Res.* **1993**, *38*, 229.
- (5) Hansson, O.; Wydrzynski, T. *Photosynth. Res.* **1990**, *23*, 131.
- (6) Michel, H.; Deisenhofer, J. *Biochemistry* **1988**, *27*, 1.

- (7) Parson, W. W. In *Chlorophylls*; Scheer, H., Ed.; CRC Press: Boca Raton, 1991; p 1153.
- (8) Eijkelhoff, C.; Dekker, J. P. *Biochim. Biophys. Acta* **1995**, *1231*, 21.
- (9) Vacha, F.; Joseph, D. M.; Durrant, J. R.; et al. *Proc. Natl. Acad. Sci. U.S.A.* **1995**, *92*, 2929.
- (10) Roelofs, T. A.; Kwa, S. L. S.; van Grondelle, R.; Dekker, J. P.; Holzwarth, A. R. *Biochim. Biophys. Acta* **1993**, *1143*, 147.
- (11) Roelofs, T. A.; Gilbert, M.; Shuvalov, V. A.; Holzwarth, A. R. *Biochim. Biophys. Acta* **1991**, *1060*, 237.
- (12) Schelvis, J. P. M.; van Noort, P. I.; Aartsma, T. J.; van Gorkom, H. J. *Biochim. Biophys. Acta* **1994**, *1184*, 242.
- (13) Gatzten, G.; Müller, M. G.; Griebenow, K.; Holzwarth, A. R. *J. Phys. Chem.* **1995**, in press.
- (14) Groot, M. L.; Peterman, E. J.; van Kan, P. J. M.; van Stokkum, I. H. M.; Dekker, J. P.; van Grondelle, R. *Biophys. J.* **1994**, *67*, 318.
- (15) Tang, D.; Jankowiak, R.; Seibert, M.; Yocum, C. F.; Small, G. J. *J. Phys. Chem.* **1990**, *94*, 6519.
- (16) Konermann, L.; Holzwarth, A. R. *Biochemistry* **1996**, *35*, 829.
- (17) Durrant, J. R.; Klug, D. R.; Kwa, S. L.; van Grondelle, R.; Porter, G.; Dekker, J. P. *Proc. Natl. Acad. Sci. U.S.A.* **1995**, *92*, 4798.
- (18) Wasielewski, M. R.; Johnson, D. G.; Govindjee; Preston, C.; Seibert, M. *Photosynth. Res.* **1989**, *22*, 89.
- (19) Wasielewski, M. R.; Johnson, D. G.; Seibert, M.; Govindjee. *Proc. Natl. Acad. Sci. U.S.A.* **1989**, *86*, 524.
- (20) Schatz, G. H.; Brock, H.; Holzwarth, A. R. *Proc. Natl. Acad. Sci. U.S.A.* **1987**, *84*, 8414.
- (21) Schatz, G. H.; Brock, H.; Holzwarth, A. R. *Biophys. J.* **1988**, *54*, 397.
- (22) Holzwarth, A. R.; Müller, M. G.; Gatzten, G.; Hücke, M.; Griebenow, K. *J. Lumin.* **1994**, *60/61*, 497.
- (23) Hastings, G.; Durrant, J. R.; Barber, J.; Porter, G.; Klug, D. R. *Biochemistry* **1992**, *31*, 7638.
- (24) Jankowiak, R.; Tang, D.; Small, G. J.; Seibert, M. *J. Phys. Chem.* **1989**, *93*, 1649.
- (25) Durrant, J. R.; Hastings, G.; Joseph, D. M.; Barber, J.; Porter, G.; Klug, D. R. *Biochemistry* **1993**, *32*, 8259.
- (26) Klug, D. R.; Rech, T.; Joseph, D. M.; Barber, J.; Durrant, J. R.; Porter, G. *Chem. Phys.* **1995**, *194*, 433.
- (27) Rech, T.; Durrant, J. R.; Joseph, D. M.; Barber, J.; Porter, G.; Klug, D. R. *Biochemistry* **1994**, *33*, 14768.
- (28) Durrant, J. R.; Hastings, G.; Joseph, D. M.; Barber, J.; Porter, G.; Klug, D. R. *Proc. Natl. Acad. Sci. U.S.A.* **1992**, *89*, 11632.
- (29) Müller, M. G.; Hücke, M.; Reus, M.; Holzwarth, A. R. *J. Phys. Chem.* **1996**, *100*, 9537.
- (30) van Leeuwen, P. J.; Nieveen, M. C.; van de Meent, E. J.; Dekker, J. P.; van Gorkom, H. J. *Photosynth. Res.* **1991**, *28*, 149.
- (31) McTavish, H.; Picorel, R.; Seibert, M. *Plant Physiol.* **1989**, *89*, 452.
- (32) Holzwarth, A. R.; Schatz, G. H.; Brock, H.; Bittersmann, E. *Biophys. J.* **1993**, *64*, 1813.
- (33) Holzwarth, A. R. In *Biophysical Techniques in Photosynthesis Research*; Ames, J., Hoff, A., Eds.; Kluwer Academic Publishers: Dordrecht, 1996; p 75.
- (34) Durrant, J. R.; Hastings, G.; Hong, Q.; Barber, J.; Porter, G.; Klug, D. R. *Chem. Phys. Lett.* **1992**, *188*, 54.
- (35) Renger, G. In *The Photosystems: Structure, Function and Molecular Biology*; Barber, J., Ed.; Elsevier: Amsterdam, 1992; p 45.
- (36) Danielius, R. V.; Satoh, K.; van Kan, P. J. M.; Plijter, J. J.; Nuijs, A. M.; van Gorkom, H. J. *FEBS Lett.* **1987**, *213*, 241.
- (37) van Dorssen, R. J.; Breton, J.; Plijter, J. J.; Satoh, K.; van Gorkom, H. J.; Ames, J. *Biochim. Biophys. Acta* **1987**, *893*, 267.
- (38) Gatzten, G.; Griebenow, K.; Müller, M. G.; Holzwarth, A. R. In *Research in Photosynthesis. II*; Murata, N., Ed.; Kluwer Academic Publishers: Dordrecht, 1992; p 69.
- (39) Greenfield, S. R.; Wasielewski, M. R.; Govindjee; Seibert, M. In *Photosynthesis: from Light to Biosphere*; Mathis, P., Ed.; Kluwer Academic Publishers: Dordrecht, 1995; p 663.
- (40) Wiederrecht, G. P.; Seibert, M.; Govindjee; Wasielewski, M. R. *Proc. Natl. Acad. Sci. U.S.A.* **1994**, *91*, 8999.
- (41) Bixon, M.; Jortner, J.; Michel-Beyerle, M. E. *Chem. Phys.* **1995**, *197*, 389.
- (42) Peloquin, J. M.; Williams, J. C.; Lin, X.; et al. *Biochemistry* **1994**, *33*, 8089.
- (43) Müller, M. G.; Dorra, D.; Holzwarth, A. R.; Gad'on, N.; Drews, G. In *Photosynthesis: from Light to Biosphere*. Vol. I; Mathis, P., Ed.; Kluwer Academic Publishers: Dordrecht, 1995; p 595.
- (44) Konermann, L.; Gatzten, G.; Holzwarth, A. R. *J. Phys. Chem.* **1996**, submitted for publication.
- (45) In a recent publication a 5 Chl/2 Pheo preparation has been reported.⁹
- (46) The actual experimental lifetime found was 2–3 ps. The large range of 1–6 ps for this component was based on a very conservative estimate of the error limits.
- (47) Note that the fluorescence kinetics has generally a higher S/N ratio than transient absorption data, which may rationalize the larger number of lifetime components that we found in fluorescence.
- (48) We have previously noted²⁹ that Hastings et al. might have measured the spectra in the 545 nm range at a higher excitation intensity. However this effect would still not fully explain the discrepancy.
- (49) Our suggestion is based on a comparison of the kinetics of our own measurements at 545 nm at higher excitation intensity with those of Klug et al.²⁶ and Hastings et al.²³ We note, however, that the authors claim that the excitation intensity was the same at all detection wavelengths (personal communication, J. Durrant).

JP953714I